Long-Term Evaluation of Reinforcement Effectiveness for Old and Dilapidated Bridges Based on Load Testing

Manhui Liu

Zhejiang Academy of Transportation Sciences, Hangzhou 311305, Zhejiang, China

Abstract: This study investigates the residual load-bearing capacity of an old bridge five years post-strengthening. The bridge, a T-shaped rigid frame structure with suspended spans, was constructed in 1999. Due to significant deterioration, it was rated as a Class D (Structurally Deficient) bridge in 2018 and subse-quently strengthened. Post-reinforcement load tests conducted in 2019 con-firmed compliance with design requirements. In December 2023, follow-up load tests (including static and dynamic load testing) were performed to re-assess its performance. Results indicate a significant degradation in load-carrying capacity over the intervening period. This research provides valuable insights for long-term effectiveness evaluation of reinforcement techniques on aging bridges, contributing to ensuring structural safety and serviceability.

Keywords: Aging bridge Reinforcement; Load Testing; Load-bearing Capacity

1. Introduction

With the continuous development of transportation infrastructure in China, a large number of old bridges are facing problems such as insufficient bearing ca-pacity and structural diseases. As a representative T-shaped rigid frame bridge with hanging beams, an old bridge has undergone multiple disease inspections and reinforcement designs since it was completed and opened to traffic in 1999. In 2018, the bridge was rated as a Class V dangerous bridge due to diseases such as multiple over-limit cracks and concrete damage and spalling, and then a temporary restrictive traffic maintenance and reinforcement design was carried out. The load test in January 2019 showed that the reinforced bridge was in an elastic working state under the design load, and its stiffness and strength could meet the design requirements. However, after five years of operation, whether the remaining bearing capacity can still meet the design requirements is worthy of further study. Therefore, this study inspects the bearing effect of the dangerous bridge five years after reinforcement through bridge load tests, aiming to provide a reference for the reinforcement effect evaluation of similar old bridges, so as to ensure the safe operation of bridges and extend their service life. At the same time, it also accumulates more practical experience for the bridge engineering field in the reinforcement and evaluation of old bridges.

2. Project Overview

The main bridge of an old bridge is a T-shaped rigid frame bridge with hanging beams, which

was completed and opened to traffic in May 1999. The reinforcement design was carried out in 2018, and the elevation schematic diagram of the bridge is shown in Figure 1. It has two-way two lanes, and the cross-sectional composition is: 0.25m (railing) + 1m (sidewalk) + 7m (driving lane) + 1m (side-walk) + 0.25m (railing) = 9.5m. The main piers adopt hollow thin-walled piers, and the foundation adopts bored pile foundation.

In March 2018, a regular inspection of the bridge revealed multiple diseases such as over-limit cracks in the upper and lower structures, concrete damage and spalling, deck system damage, and support deformation. Finally, it was rated as a Class V bridge, which belongs to the category of dangerous bridges. In October 2018, a temporary restrictive traffic maintenance and reinforcement design was carried out. The main reinforcement methods were external prestressing reinforcement in the negative moment area of the T-frame (as shown in Figure 2) and steel plate pasting reinforcement on the outer side of the web of the main bridge cantilever box girder (as shown in Figure 3), with heavy vehicle passage restricted. The design traffic load standard for reinforcement is: a special road for small vehicles, using Steam-10 load, and a pedestrian load of 3.5KPa. In January 2019, a load test was conducted on the reinforced bridge. The test conclusion was that under the design load, it was in an elastic working state, and its stiffness and strength could meet the design requirements. In August 2022, a regular inspection of the bridge rated it as a Class 3 bridge. In December 2023, a study on the remaining bearing capacity of the bridge was carried out to inspect the bearing effect of the dangerous bridge five years after reinforcement. The study was conducted through a bridge load test.

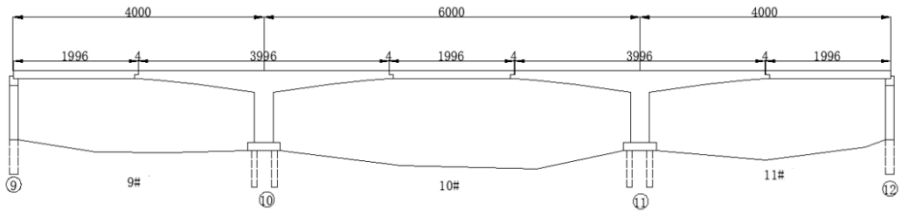

Figure 1: Elevation Schematic Diagram of an Old Bridge.

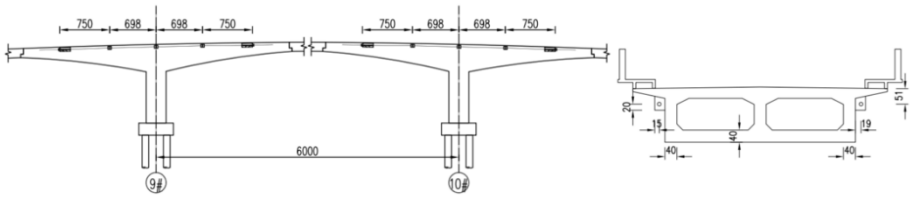

Figure 2: Diagram of External Prestressing Reinforcement.

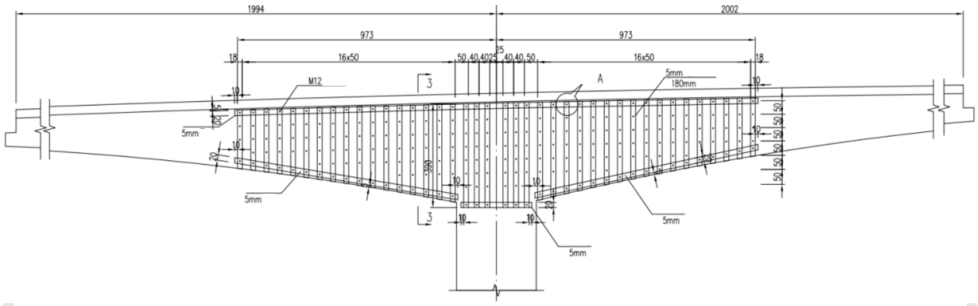

Figure 3: Diagram of Steel Plate Pasting Reinforcement.

3. Purpose and Content of Load Testing

3.1 Purpose of Load Testing

This study aims to understand the remaining bearing capacity of the old bridge five years after the reinforcement construction and operation, so as to provide a reference for the evaluation of the reinforcement effect of old bridges.

3.2 Content of Load Testing

Bridge load testing is typically categorized into static load tests and dynamic load tests. The static load test primarily involves measuring strain and deflection at critical sections under static loading conditions, while inspecting key cross-sections of the main girders for crack initiation. Should cracks be observed, their propagation behavior is monitored in real-time during testing. The dynamic load test focuses on measuring the structure's natural vibration frequencies and damping ratios under dynamic excitation. Ultimately, field-measured static and dynamic test data are analyzed alongside theoretical calculations to comprehensively evaluate the bridge's load-bearing capacity and serviceability performance [1-2].

4. Static Load Test

4.1 Theoretical Calculation

The calculation and analysis are carried out by using the special finite element analysis software MIDAS, and the analysis model is shown in the following figure. The T-beams are simulated by the grid method, and the T-structures are simulated by single beams [3]. The full-bridge model includes 446 nodes and 578 beam elements, as shown in Figure 4.

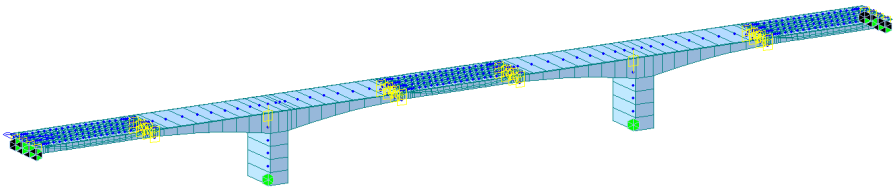

Figure 4: Finite Element Modeling.

4.2 Test Sections and Instrumentation Layout

According to the mechanical characteristics of the rigid frame bridge and finite element calculations, the main control sections of the structure were selected for the static load test. The L/2 section of the 9th span, the L/3 section of the 10th span, and the section near the top of Pier 10 were selected as the test control sections. The control sections of the bridge are shown in Figure 5, and the test contents of the control sections are listed in Table 1.

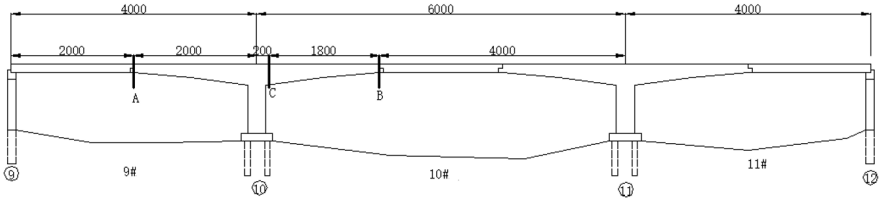

Figure 5: Finite Element Modeling.

Table 1: Test Contents of Control Sections.

Designated Sections	Position	Test Parameters
A	Midspan of Span 9 (L/2 section)	Deflection
B	Section at L/3 of Span 10	Deflection
C	Negative Moment and Shear Sections in the Vicinity of Pier #10	Strain

The arrangement of deflection sensors is shown in Figure 6, and the arrangement of strain measuring points is shown in Figure 7.

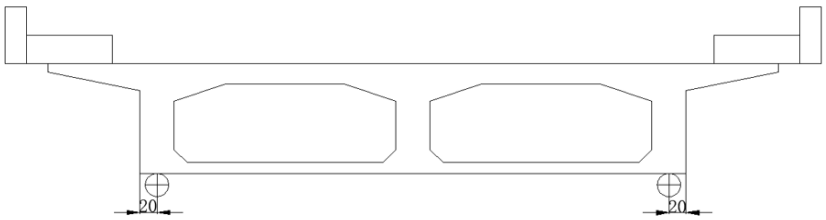

Figure 6: Schematic Diagram of Deflection Sensor Arrangement.

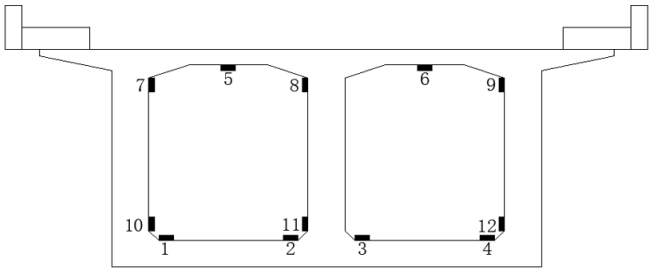

Figure 7: Schematic Diagram of Strain Sensor Arrangement.

4.3 Load Test Cases

The load test was carried out using four three-axle vehicles each with a weight of 220 kN. The front axle weighed 60 kN, and the dual rear axles weighed 160 kN. Due to the narrow width of the bridge deck, the loading positions for eccentric loading and central loading were close to each other. Therefore, only the eccentric loading condition was adopted in this test:

Condition 1: Maximum deflection at Section A of 1/2L in Span 9 (eccentric loading);

Condition 2: Maximum deflection at Section B of 1/3L in Span 10 (eccentric loading);

Condition 3: Negative moment at Section C near Pier 10 (eccentric loading);

Condition 4: Shear force at Section C of T-structure (eccentric loading).

The loading efficiency ranges from 0.95 to 1.05 based on the principle of load equivalence, and the loading diagrams are shown in Figures 8-9.

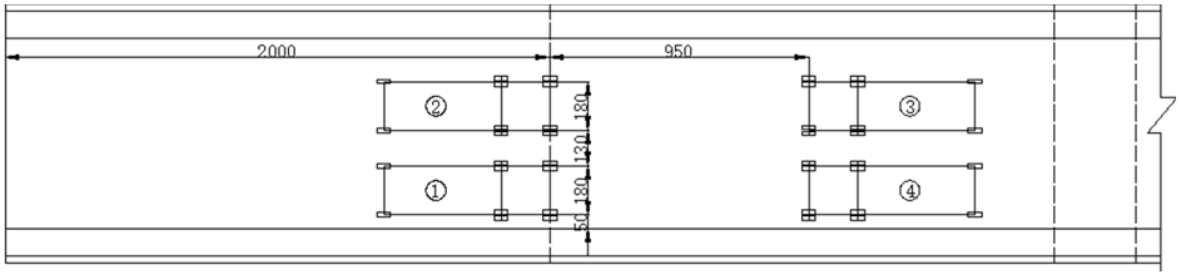

Figure 8: Loading Diagram of Condition 1

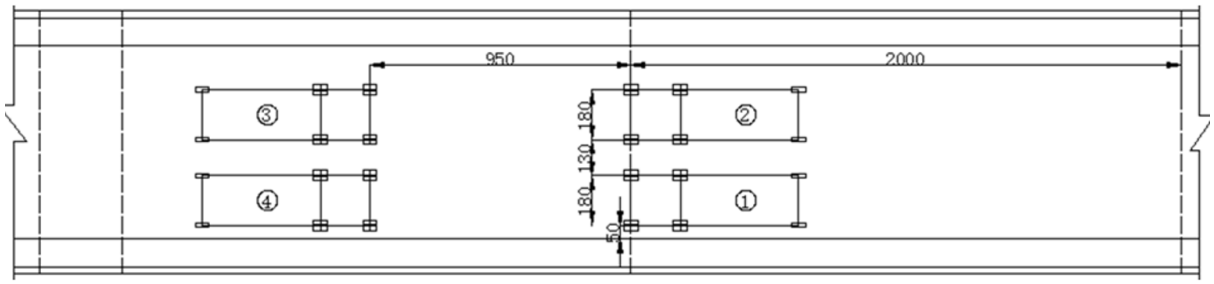

Figure 9: Loading Diagrams of Conditions 2, 3 and 4

The test was originally planned to be loaded in four stages, namely Stage 1: Vehicle No. 1; Stage 2: Vehicles No. 1-2; Stage 3: Vehicles No. 1-3; Stage 4: Vehicles No. 1-4, with one-time unloading. During the on-site implementation, it was found that when the loading reached the second stage, the measured deflection value far exceeded the theoretical value of the second-stage loading, so the loading was stopped.

4.4 Test Results and Analysis

The comparison results between the deflection values of each test section and the theoretical calculation values under each load condition are shown in Tables 2-3:

Table 2: Condition 1 Maximum Deflection of Section A at 1/2L of Span 9 (Eccentric Loading).

Deflection Measuring Point		The second-stage measured value(mm)	Residual Deflection (mm)	Maximum Elastic Deformation ①(mm)	Theoretical Calculated Value②(mm)	Check Coefficient η①/②	Average Check Coefficient	Relative Residual (%)
A	1#	-15.6	-0.3	-15.3	-10.8	1.41	1.42	2.1
	2#	-15.9	-0.4	-15.5	-10.8	1.43		2.4

Table 3: Condition 2 Maximum Deflection at Section B of 1/3L in Span 10 (Eccentric Loading).

Deflection Measuring Point		The second-stage measured value(mm)	Residual Deflection (mm)	Maximum Elastic Deformation①(mm)	Theoretical Calculated Value②(mm)	Check Coefficient η①/②	Average Check Coefficient	Relative Residual (%)
B	1#	-15.2	-0.5	-14.7	-10.8	1.36	1.37	3.0
	2#	-15.4	-0.5	-15.0	-10.8	1.39		3.1

The comparison results between the strain values of the test sections near the pier top and the theoretical calculation values under each load condition are shown in Table 4:

Table 4: Condition 3 Negative Moment at Section F near Pier 10 (Eccentric Loading).

Deflection Measuring Point		The second-stage measured value(mm)	Residual Deflection (mm)	Maximum Elastic Deformation (mm)	Average value of maximum elastic strain ① (με)	Theoretical calculation value ② (με)	Average Check Coefficient①/②	Relative Residual (%)
1		-16.3	0.5	-16.8				-3.0
2	Bottom	-15.3	-1.4	-13.9	-20.6	-43.0	0.48	9.4
3	Plate	-22.8	1.6	-24.4				-7.1
4		-27.8	-0.5	-27.3				1.7
5	Top	1.4	-7.7	9.1	4.8	33.0		-535.7
6	Plate	4.8	4.3	0.5				90.0
7	Upper	5.3	-0.5	5.7				-9.1
8	Web	2.9	-1.4	4.3	7.2	28.0	/	-50.2
9	Plate	10.1	-1.4	11.5				-14.2
10	Lower	-55.0	-32.5	-22.5				59.1
11	Web	9.6	14.8	-5.3	-18.0	-32.0		155.0
12	Plate	7.2	33.5	-26.3				466.6

The last load test of this bridge was conducted in 2019, with the maximum loading capacity being 20t (two 10t loading vehicles). The first-stage loading of this test is one 22.5t loading vehicle, and the loading weight and position are similar to those of the last test. Therefore, it is considered that the first-stage loading of this test is comparable to the results of the last test. The comparison of the test conditions between the two tests is shown in Table 5.

Table 5: Comparison of Load Test Conditions in 2019 and 2023.

Serial Number	Condition	Test Results in 2019			Test Results in 2023		
1	Deflection of 9# Span L/2 Section (Medium Load)	Theoretical Average Value(mm)	-5.02	0.97	Theoretical Average Value(mm)	-5.10	1.46
		Measured Average Value(mm)	-4.85		Measured Average Value(mm)	-7.45	
2	Deflection of 10# Span L/3 Section (Medium Load)	Theoretical Average Value(mm)	-4.46	0.96	Theoretical Average Value(mm)	-5.10	1.44
		Measured Average Value(mm)	-4.30		Measured Average Value(mm)	-7.36	

The test scheme of the bridge was formulated according to four-stage loading. During on-site

loading, it was found that after loading two vehicles, the measured deflection data exceeded the corresponding graded theoretical value and the theoretical ultimate loading value, so the loading was stopped. Finally, the second-stage loading was adopted, in which the loading efficiency of the deflection condition was 0.75, and the loading efficiency of the negative moment condition was 0.71.
Under the action of the test load, the average check coefficient of the deflection condition at the cantilever end of the T-structure of Qixing Bridge was 1.35-1.45, both greater than 1.00; the maximum relative residual strain was 3.9%, which did not exceed 20%, indicating that the stiffness did not meet the specification requirements, but it was still in the elastic working state.

According to the on-site appearance inspection, there are multiple transverse cracks (repaired), longitudinal cracks at the position near the pier top of the box girder roof, the inner bottom plate of the box girder is uneven, and the web is covered with reinforcing steel plates. There is a large gap between the parameters such as the integrity of the box girder section, the actual flexural stiffness, and the position of the neutral axis and the theoretical calculation, so the measured strain results of the T-structure are only for reference [4-5]. Under the action of the test load, the average check coefficient of the negative moment condition is 0.48, and the relative residual strain is generally large.
Compared with the results of the 2019 load test, the average check coefficient of the deflection condition in 2019 was 0.96-0.98, and that in 2023 was 1.40-1.55, which increased significantly. This indicates that the bridge stiffness has been significantly weakened.

5. Dynamic Load Test

5.1 Test Content

The dynamic characteristics (mode shapes, frequencies, damping ratios, impact coefficients) of bridge structures are important parameters for evaluating bridge bearing capacity, and also important parameters for identifying the working performance of bridge structures and seismic analysis of bridges. The main dynamic parameters of the bridge structure tested this time include: structural mode shape (fundamental frequency), damping ratio, impact coefficient, etc.
The theoretical calculation models for the dynamic load test all adopt the calculation models established in the static load test. Through calculation, the first-order vertical vibration frequency of the bridge is shown in the following table, and the mode shape is shown in Figure 10.

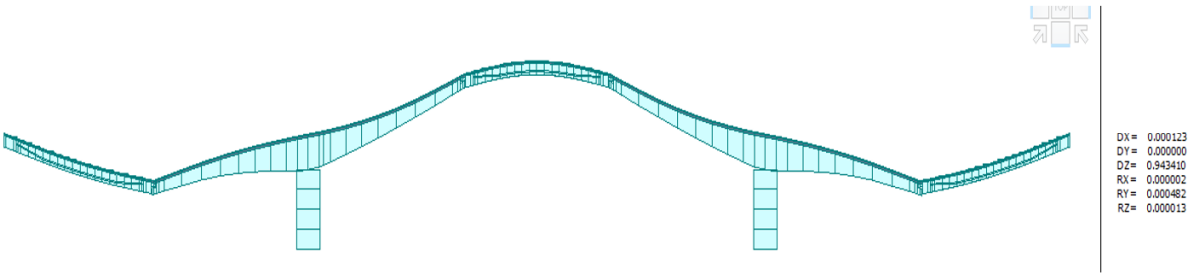

Figure 10. First-order vertical vibration mode diagram (f1=1.921Hz)

5.2 Test Results and Analysis Comparison

The comparison between the measured frequency and the theoretical calculated value of the dynamic test for Qixing Bridge is shown in Table 6.

Table 6: Comparison between Calculated Fundamental Frequency and Measured Frequency in Dynamic Load Test.

Modal Order	Measured Value f_{di} （Hz）	Theoretical Calculation Value f_{di} (Hz)	Damping Ratio
First Order	1.514	1.921	0.033

It can be seen from the above table that the measured first-order vibration frequency value of the test span is smaller than the theoretical calculated value, indicating that the vertical stiffness of the structure reflected by the measured results is smaller than that reflected by the theoretical calculation, and the overall dynamic stiffness of the test span does not meet the specification requirements. The test results of the impact coefficient under different vehicle speeds are shown in Figures 11-12, and the comparison between the measured values and the theoretical calculated values is shown in Table 7.

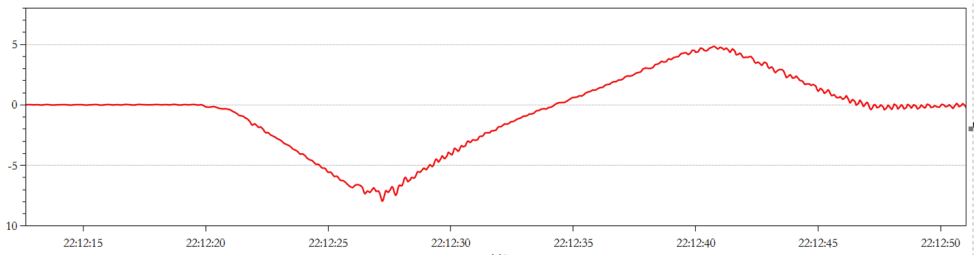

Figure 11: Impact Coefficient at a Speed of 10 km/h: 1+μ=1.061.

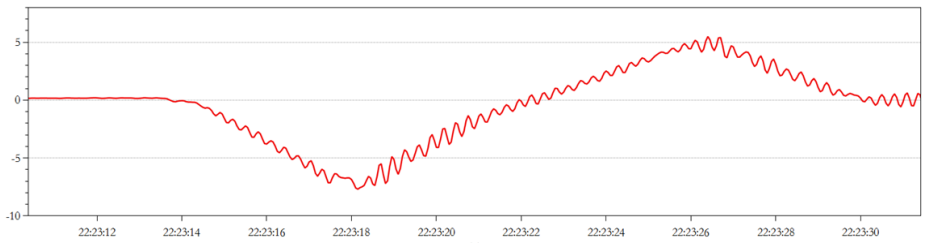

Figure 12: Impact Coefficient at a Speed of 20 km/h: 1+μ=1.140.

Table 7: Comparison Between Measured Impact Coefficients and Calculated Values Specified in Codes.

Driving Speed	Impact Coefficient (1+μ)	
	Measured Value	Theoretical Value
10km/h	1.061	1.100
20km/h	1.140	

It can be seen from Table 7 that when the test vehicle travels at 20 km/h, the measured impact coefficient of the test span structure exceeds the calculated value by the specification method.

6. Conclusion

The strain results in the load test reflect the local conditions of the strain gauge. For old bridges

with widespread cracks, they are easily affected by factors such as the layout position and the stiffness change of the cracked section. In comparison, the deflection condition of the static load test can better reflect the overall stiffness of the bridge.

Through the comparison of the static load test results in 2019 and 2023, it can be seen that the bearing capacity of the old bridge has significantly decayed after 5 years of reinforcement.

The results of the 2023 dynamic load test are consistent with those of the static load test, indicating that the bearing capacity of the bridge fails to meet the requirements.

References

[1] Liu Liang, Wu Jinhua, Zhang Baojun. Load test analysis of continuous rigid frame bridges. Hunan Communication Science and Technology, 2010, 36(3): 59-62.

[2] Song Yifan. Load Tests and Structural Evaluation of Highway Bridges. China Communications Press, 2002.

[3] Chen Hao. Comparative Study on Detection and Evaluation Methods for Bridge Engineering. Engineering and Construction, 2023, 37(6): 1751-1752, 1805. DOI: 10.3969/j.issn.1673-5781.2023.06.033.

[4] Weiwei Lin,2018，Rehabilitation and Strengthening of Aged Steel Railway Bridges in Japan,Journal of Civil & Environmental Engineering,DOI: 10.4172/2165-784X.1000305.

[5] Matos, J. C., Nicoletti, V., Kralovanec, J., Sousa, H. S., Gara, F., Moravcik, M., & Morais, M. J. (2023) Comparison of Condition Rating Systems for Bridges in Three European Countries. Appl. Sci. 2023,13, 12343. https://doi.org/10.3390/app132212343.